https://doi.org/10.5194/egusphere-2026-4017
Preprint. Discussion started: 28 July 2026

Concurrent Heat and Intense UV Extremes in North America: Divergent Dynamical Drivers and Exacerbated Ozone Pollution

Binbin Bao[1], Yan Xia[1], Fei Xie[1]

[1]School of Systems Science, Beijing Normal University, Beijing, 100875, China

Correspondence to: Yan Xia (xiayan@bnu.edu.cn)

Abstract. The co-occurrence of extreme heat and intense ultraviolet (UV) radiation poses severe yet insufficiently understood threats to terrestrial ecosystems and public health. Using reanalysis datasets from 1940 to 2022, we reveal the spatiotemporal characteristics and driving mechanisms of compound summer heat-UV events across North America. We identify two primary hotspots: the southwestern United States to northern Mexico, and central-western Canada to the northwestern United States. Dynamically, these events are anchored by anomalous anticyclonic circulations—specifically, the westward expansion of the North Atlantic Subtropical High in the south, and mid-latitude high-pressure ridges in the north. These persistent systems trigger severe soil desiccation, subsidence warming, and significant cloud reductions (up to ~13 %), synergistically amplifying surface temperature and solar UV flux. Furthermore, we demonstrate that this compound extreme substantially accelerates tropospheric photochemical processes, leading to a marked increase in surface ozone concentrations (up to 15.91 ppbv) and shifting the probability distribution toward extreme pollution episodes, primarily in the southern hotspot. Since 1980, the frequency of these compound events has increased significantly by 1.29 events per decade. The significant upward trend of these compound events highlights an intensifying climate-environmental hazard, underscoring the necessity of integrating combined heat, UV, and ozone risks into regional public health and pollution mitigation strategies.

1 Introduction

Extreme weather events, driven by global climate change, have become increasingly frequent and pose profound challenges to human society and ecosystems (Adrian et al., 2022; Campbell et al., 2018; Gulev et al., 2021; Coumou and Rahmstorf, 2012). While significant increases have been observed globally in individual extremes such as heatwaves and heavy precipitation (Perkins-Kirkpatrick and Lewis, 2020; Perkins et al., 2012; Fischer and Knutti, 2016; Papalexiou and Montanari, 2019; Chiang et al., 2021), a frontier topic in climate risk research is the emergence of compound extreme events. Formed by the simultaneous or sequential occurrence of multiple extremes, compound events pose substantially greater risks due to non-linear "1 + 1 > 2" amplification effects (Zscheischler et al., 2018; Afroz et al., 2023).

North America is a critical hotspot for such extremes, characterized by warming rates exceeding the global land average and a high level of societal exposure (USGCRP, 2018; Perkins, 2015; Grotjahn et al., 2016; Philip et al., 2022). The escalating

https://doi.org/10.5194/egusphere-2026-4017
Preprint. Discussion started: 28 July 2026

frequency and intensity of extreme heat in this region have driven severe multidisciplinary impacts. These include sharp increases in excess mortality and healthcare pressure (Anderson and Bell, 2010; Knowlton et al., 2008), reductions in outdoor labor productivity (Graff Zivin and Neidell, 2014), non-linear declines in major crop yields (Schlenker and Roberts, 2009), and intensified forest mortality and wildfire risks (Allen et al., 2010; Westerling et al., 2006). Rapid urbanization further intensifies these vulnerabilities, particularly in metropolitan areas facing population growth and urban heat island effects (Jones et al., 2015).

The physical mechanisms underlying extreme heat in North America exhibit a multi-scale synergy. At the circulation level, events are predominantly triggered by the anomalous westward extension of the North Atlantic Subtropical High (NASH) (Li et al., 2012; Li et al., 2019) and quasi-stationary mid-latitude planetary wave trains (Teng et al., 2013). These persistent high-pressure ridges, clearly identifiable in the 500-hPa geopotential height field (Adams et al., 2021; Loikith and Broccoli, 2012), strongly suppress convection, resulting in reduced cloud cover and subsidence warming (Grotjahn et al., 2016). Concurrently, severe soil desiccation alters surface energy partitioning, creating a positive land-atmosphere feedback loop that critically amplifies surface heating (Seneviratne et al., 2010; Miralles et al., 2014).

Despite a robust understanding of the aforementioned processes, most existing studies have focused primarily on single heat events or compound heat-drought extremes. A novel and highly destructive compound event—the concurrent occurrence of extreme heat and strong ultraviolet (UV) radiation—has been recently identified over the Yangtze Plain in China during summer (Xia et al., 2022). However, systematic investigations of such events remain critically limited in North America. The persistent clear-sky conditions dictated by the NASH and mid-latitude westerlies inherently amplify incoming solar UV radiation simultaneously with surface heating.

This concurrence represents a severe coupled climate-environment stressor. Ecologically, combined heat and UV exposure can non-linearly intensify plant photoinhibition and disrupt terrestrial carbon sinks (Bornman et al., 2019; Robson et al., 2022; Liaqat et al., 2024; Häder et al., 2015; Ballaré et al., 2011). Environmentally, elevated temperatures and strong UV radiation synergistically accelerate atmospheric photochemical processes, substantially increasing the risk of surface ozone pollution (Xia et al., 2022; Jacob and Winner, 2009; Schnell and Prather, 2017; Fiore et al., 2012; Madronich et al., 2023). This issue is particularly relevant given the persistent ozone pollution challenges in many North American metropolitan and agricultural areas (Lu et al., 2026), alongside the amplified health risks for vulnerable populations exposed to combined heat stress and UV damage (Zhao and Yang, 2025; World Health Organization, 2017).

While the intensity of surface UV radiation is governed by stratospheric ozone (Bais et al., 2015) and tropospheric factors like cloud cover and aerosols (Williamson et al., 2014; Barnes et al., 2019), recent studies have highlighted the profound regional importance of circulation-induced cloud effects on UV levels (Xia et al., 2021a; Xia et al., 2021b). This raises a critical scientific question: Does the anomalous westward extension of the NASH or other synoptic systems systematically modify cloud conditions over North America, thereby driving compound heat-UV extremes? Given the continent's large population and status as a vital global food producer (Dyson, 1999), addressing this question is imperative.

https://doi.org/10.5194/egusphere-2026-4017
Preprint. Discussion started: 28 July 2026

Based on the above considerations, this study aims to: (a) identify the spatiotemporal characteristics of compound heat-UV events in North America; (b) reveal their dominant atmospheric circulation mechanisms; (c) evaluate their impacts on surface ozone pollution; (d) analyze their long-term trends. The following sections describe the data, methodology, and results in detail.

2 Data and methods

2.1 Data

Datasets used in this study include the ERA5 reanalysis, ERA5-Land reanalysis, and the CAMS atmospheric composition reanalysis. The ERA5 and ERA5-Land data are publicly available from the Copernicus Climate Data Store (CDS) (Hersbach et al., 2020; Muñoz-Sabater et al., 2021). The CAMS EAC4 data are publicly available from the Copernicus Atmosphere Data Store (ADS) (Inness et al., 2019).

Monthly mean variables from the ERA5 reanalysis dataset were used for the period 1940–2022, including 2 m air temperature, surface solar ultraviolet radiation, total precipitation, geopotential height, total column ozone, and cloud cover at different levels (total, high, medium, and low). These variables have a horizontal resolution of 0.25° × 0.25°. In addition, monthly mean volumetric soil water content in the surface layer from the ERA5-Land reanalysis dataset was used for the period 1950–2022, with a horizontal resolution of 0.1° × 0.1°.

Both ERA5 and ERA5-Land are generated using an advanced four-dimensional variational data assimilation (4D-Var) system within the Integrated Forecasting System (IFS) of the European Centre for Medium-Range Weather Forecasts (ECMWF). This system combines multi-source observational data with model simulations to produce optimal global estimates of atmospheric and land-surface states (Hersbach et al., 2020; Muñoz-Sabater et al., 2021). In the ERA5 dataset, solar ultraviolet radiation is defined as radiation within the wavelength range of 200–440 nm.

To examine the influence of concurrent extreme heat and intense ultraviolet radiation on surface ozone, monthly mean surface ozone from the CAMS atmospheric composition reanalysis (EAC4) was used for the period 2003–2022 at a horizontal resolution of 0.75° × 0.75°. The EAC4 reanalysis is also produced using a four-dimensional variational data assimilation (4D-Var) system that integrates global observations with model simulations to provide a temporally consistent and globally coherent estimate of atmospheric composition (Inness et al., 2019). Owing to its robust representation of tropospheric photochemical processes, the EAC4 dataset has been extensively applied in recent assessments of near-surface ozone variability and pollution extremes (Liao et al., 2025; Niu et al., 2025; Wang et al., 2025).

In addition, daily noon-time averages (UTC 18:00–20:00) of 2 m air temperature and surface solar ultraviolet radiation from the ERA5 reanalysis were used for the period 1980–2022 to analyze the long-term variability of extreme weather events.

https://doi.org/10.5194/egusphere-2026-4017
Preprint. Discussion started: 28 July 2026

2.2 Methods

We employed a composite analysis approach to investigate concurrent extreme heat and intense ultraviolet (UV) radiation events during summer over North America. The analysis focuses on two key regions: a northern center (45° N–55° N, 85° W–120° W) and a southern center (25° N–40° N, 97.5° W–107.5° W), as indicated by the black boxes in Fig. 1. Composite analysis has been widely used in previous studies to examine the characteristics and mechanisms of climate extremes (Xia et al., 2022; Xia et al., 2021a; Xie et al., 2016; Xie et al., 2017; Xie et al., 2020; Xiang et al., 2025).

This study focuses on climate extreme events, which are defined based on whether the area-weighted spatial mean over the study region exceeds a specified threshold. A monthly extreme high-temperature event is identified when the monthly mean 2 m air temperature in a given year exceeds the climatological mean plus one standard deviation for that month. In such cases, the corresponding year is classified as a hot year for that month. The same criterion is applied to other variables (Fig. S1). To identify hot years, we focus on interannual variability by removing the linear trend from each monthly time series. Composite anomalies are calculated as the differences between the mean state during extreme high-temperature events and the climatological mean. Statistical significance is evaluated using the Student's t-test at the 95 % confidence level.

In addition, we calculated the annual number of days with extreme high temperature and intense UV radiation during summer using daily data and analyzed their trends over the period 1980–2022. A hot day is defined as a day when the daily 2 m air temperature exceeds the 90th percentile threshold, and an intense UV radiation day is defined similarly based on the 90th percentile of daily surface UV radiation. To further explore the spatiotemporal relationship between these two types of extreme events, we also counted the number of days when both events occurred simultaneously. Compound extreme events involving both high temperature and intense UV radiation can significantly increase ecological risks and the severity of environmental impacts compared with single extreme events, highlighting the importance of their investigation.

3 Result

3.1 Spatiotemporal Identification of Compound Heat-UV Hotspots

Spatial correlation analysis between summer 2 m air temperature and surface solar UV radiation during 1940–2022 reveals widespread positive correlations across most of North America (Fig. 1). Based on these spatial patterns, two primary hotspot regions characterized by concurrent extreme heat and intense UV radiation are identified. The maximum positive correlation coefficients reach 0.84 in June (Fig. 1a), 0.84 in July (Fig. 1b), and 0.83 in August (Fig. 1c). Furthermore, a comparison of these correlations across two distinct periods (1940–1980 and 1981–2022) confirms that these two strong positive correlation centers (highlighted by black boxes) remain remarkably stable over the long term (Fig. S2). This robust spatiotemporal coherence is not merely a statistical artifact; rather, it strongly implies a shared large-scale dynamic driver. It suggests that persistent synoptic systems, such as anticyclonic circulations, likely govern these regions by simultaneously clearing tropospheric clouds (maximizing incoming UV flux) and inducing adiabatic subsidence (amplifying surface heating).

https://doi.org/10.5194/egusphere-2026-4017
Preprint. Discussion started: 28 July 2026

Consequently, these persistently stable regions serve as ideal natural laboratories for investigating the physical mechanisms of compound extremes.

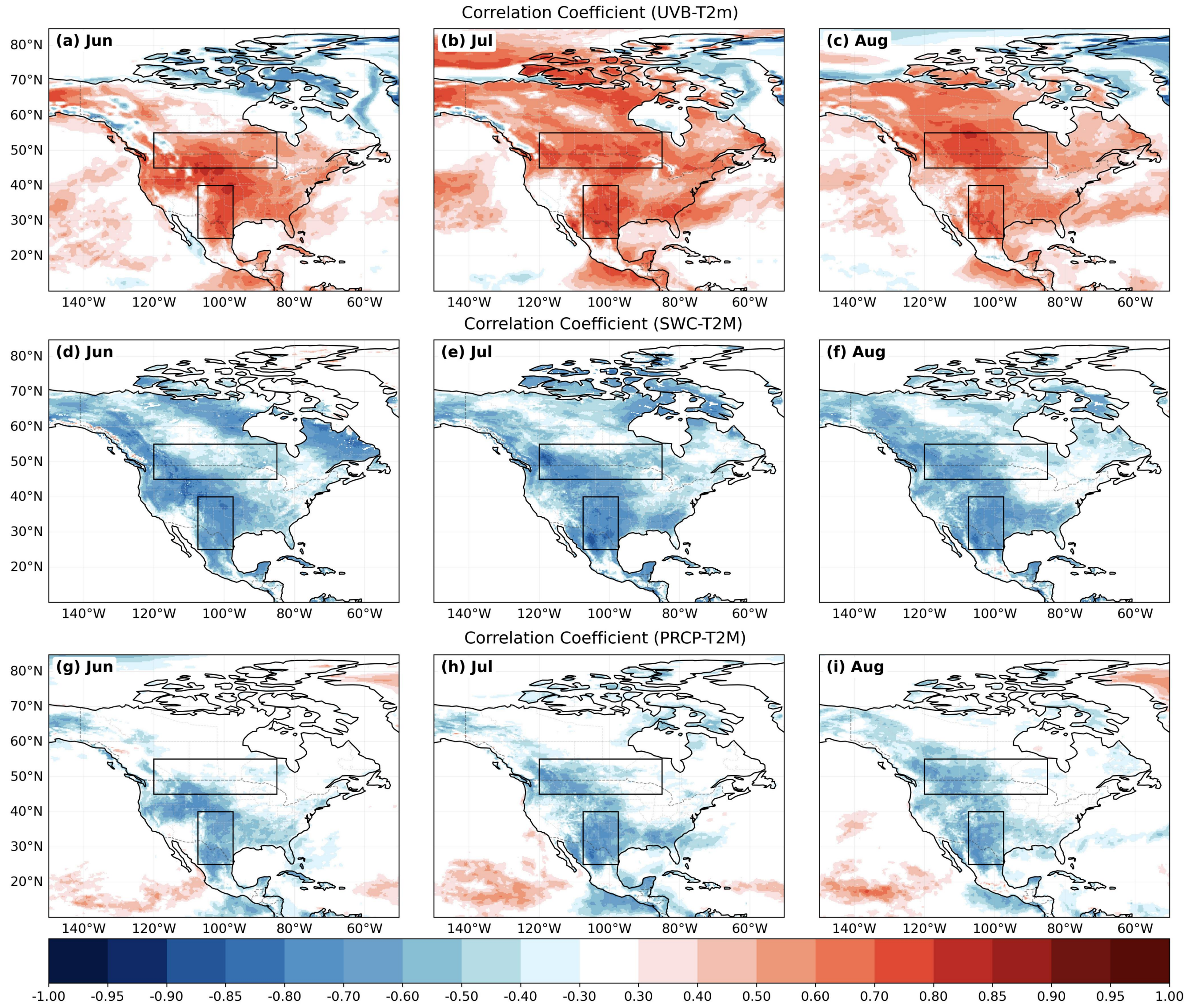

Figure 1: Spatial distributions of correlation coefficients between 2 m air temperature (T2M) and surface solar ultraviolet radiation (UVB) (a-c), total precipitation (PRCP) (g-h) during 1940 – 2022, and between 2 m air temperature and surface volumetric soil water content (d-f) during 1950–2022 at each grid point, based on monthly ERA5 and ERA5-Land reanalysis data. The black boxes indicate the northern center (45° N–55° N, 85° W–120° W) and the southern center (25° N–40° N, 97.5° W–107.5° W), respectively. The month corresponding to each panel is labeled in the upper-left corner. Correlation coefficients exceeding ± 0.3 correspond to approximately the 99.5 % confidence level for a sample size of 83 years.

Notably, these two heat-UV hotspots also spatially coincide with regions highly prone to compound heat-drought events. A pronounced negative correlation exists between 2 m air temperature and surface volumetric soil water content, with the

https://doi.org/10.5194/egusphere-2026-4017
Preprint. Discussion started: 28 July 2026

strongest negative correlations reaching -0.89 in June (Fig. 1d), -0.89 in July (Fig. 1e), and -0.85 in August (Fig. 1f). Similarly, temperature is strongly anti-correlated with total precipitation, exhibiting maximum coefficients of -0.80 in June (Fig. 1g), -0.84 in July (Fig. 1h), and -0.78 in August (Fig. 1i). Interestingly, these relationships are markedly stronger in the southern center compared to the northern center. This regional contrast suggests that the relative importance of underlying driving mechanisms may differ between the two hotspots. Specifically, the exceptionally strong negative correlations in the southern region point to a more prominent role of local land-atmosphere interactions (e.g., soil moisture-temperature feedbacks) in amplifying surface heat. In contrast, the relatively weaker hydrological coupling in the northern region implies a potentially greater dependence on large-scale atmospheric circulation anomalies. This spatial heterogeneity highlights the necessity for a differentiated dynamical analysis, which will be further detailed in the subsequent sections.

3.2 Divergent Circulation Mechanisms Driving the Northern and Southern Hotspots

During extreme heat years, composite analysis reveals that both the northern and southern hotspots experience a robust compound anomaly pattern: significantly elevated temperatures, intensified UV radiation, severe soil desiccation, and suppressed precipitation (Figs. 2 and 3). Despite these shared characteristics, the two regions exhibit notable differences in the magnitude and spatial configuration of these anomalies.

In the northern hotspot, extreme heat and enhanced UV radiation are strongly synchronized from June to August. Maximum 2 m air temperature anomalies (reaching 2.95 K, 2.77 K, and 3.01 K, respectively) geographically coincide with surface UV enhancements of 2.96 W m^{-2}, 2.95 W m^{-2}, and 2.37 W m^{-2} (Figs. 2a-f). Concurrently, this region suffers from pronounced hydroclimatic deficits. Maximum reductions in surface soil moisture reach -50 %, -84 %, and -52 %, alongside corresponding precipitation decreases of -3.19 mm, -2.00 mm, and -1.88 mm (Figs. 2g-l). These localized negative anomalies firmly confirm the widespread prevalence of drought conditions that systematically accompany extreme heat.

The southern hotspot displays an even more intense compound signature, highlighting a fiercely coupled heat-drought feedback loop. Temperature anomalies peak at 3.52 K in June — markedly stronger than the northern center — alongside simultaneous UV radiation increases of up to 2.78 W m^{-2} (Figs. 3a-f). Most strikingly, the southern region experiences exceptionally severe soil moisture depletion, plunging by -88 % in June, which far exceeds the deficit observed in the north during the same period. This extreme early-summer desiccation is accompanied by substantial precipitation deficits, reaching a maximum reduction of -4.00 mm in August. The near-perfect spatial overlap between these precipitation deficits and the warming centers underscores a tighter, more synergistic coupling between heat and drought in this southern region.

Spatially, this intense coupling of extreme heat and UV radiation is predominantly anchored within the two identified hotspots, mirroring the compound dynamics recently reported over the Yangtze Plain in China (Xia et al., 2022). However, this synchronization is not continent-wide. At higher latitudes (60° N – 70° N), temperature and UV anomalies become spatially decoupled. This distinct spatial heterogeneity underscores that the co-occurrence of these extremes is not merely a ubiquitous byproduct of uniform global warming. Rather, it is a highly localized phenomenon strictly dependent on specific, favorable synoptic environments that can simultaneously suppress cloud cover and enforce subsidence warming.

https://doi.org/10.5194/egusphere-2026-4017
Preprint. Discussion started: 28 July 2026

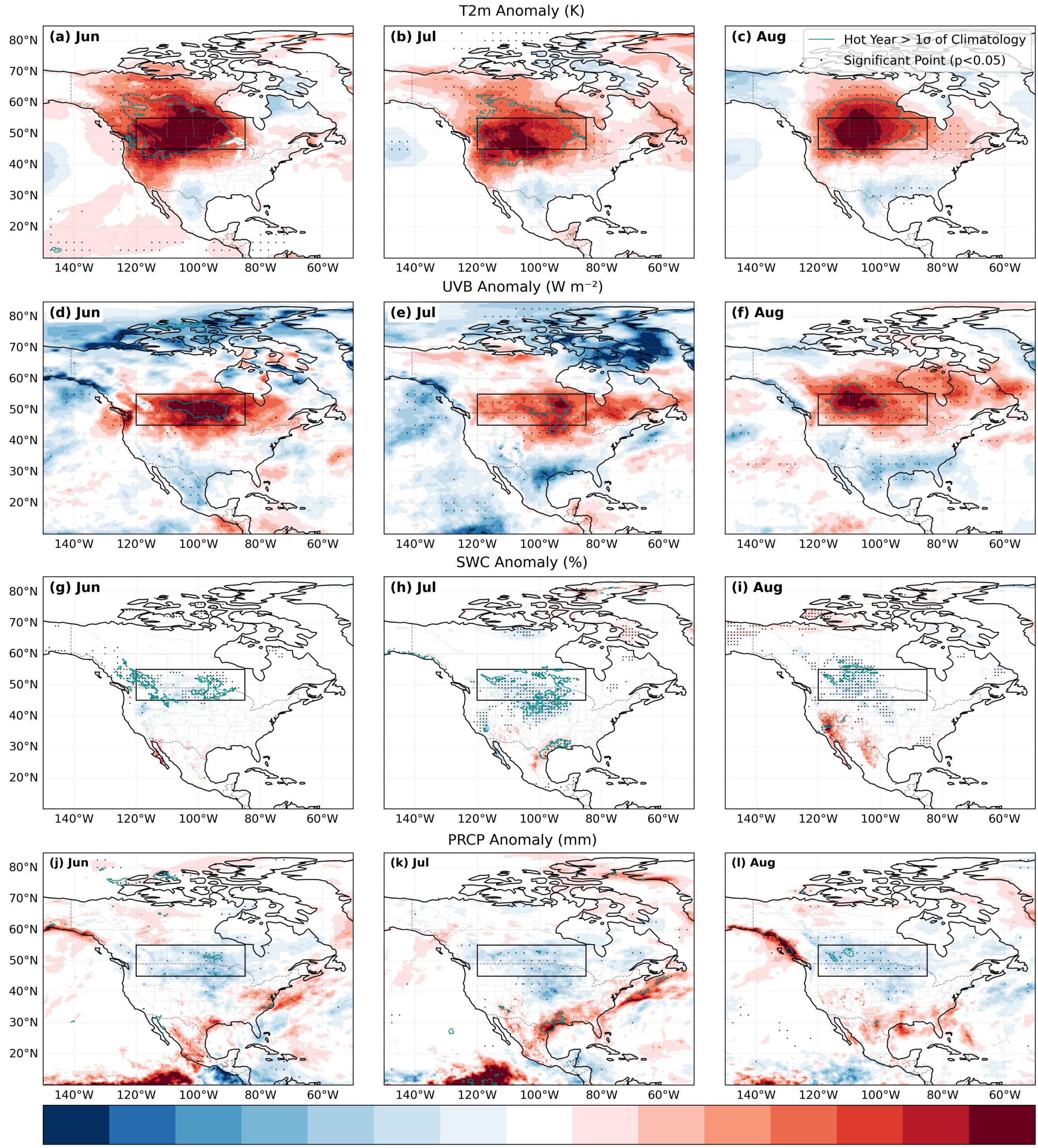

Figure 2: Spatial distributions of composite anomalies during extreme heat events in the northern center for June-August based on ERA5 reanalysis data. Panels (a-c) show 2 m air temperature (T2m) (unit: K), (d-f) surface solar ultraviolet radiation (UVB) (unit:

https://doi.org/10.5194/egusphere-2026-4017
Preprint. Discussion started: 28 July 2026

W m⁻²), and (j-l) total precipitation (PRCP) (unit: mm), with a color scale ranging from ±2.4. Panels (g-i) show surface volumetric soil water content (SWC) (unit: %), with a color scale ranging from ±80. White denotes zero, and the color scale intervals are evenly spaced. Dotted regions indicate that the composite anomalies are statistically significant at the 95 % confidence level. The dark cyan contour outlines areas where the mean values during hot years exceed ±1 standard deviation of the climatological mean.

Interestingly, these localized compound thermal events are systematically accompanied by a "seesaw-like" hydroclimatic dipole, where profound desiccation in the primary warming center contrasts with localized wet anomalies on its periphery(Figs. 2g-l, 3g-l). This spatial compensation highlights a complex dynamic interplay. Dynamically, this dipole-like configuration is likely driven by subsidence compensation mechanisms. When a region is dominated by an intense high-pressure ridge that induces desiccation, the strong descending air forces compensatory ascending motion along the periphery of the ridge, thereby promoting localized precipitation in adjacent areas (Staten et al., 2018). Additionally, the energy dispersion associated with Rossby wave trains can trigger secondary circulations that further shape this moisture dipole (Teng and Branstator, 2017). While these dipole structures are localized, recognizing such asymmetric hydroclimatic responses is crucial. It implies that the dynamic intensification of compound extremes in a core region may paradoxically alter the hydrological balance of adjacent areas.

To fundamentally understand these coupled surface anomalies, we investigate their large-scale dynamic drivers by examining composite anomalies of 500-hPa geopotential height and total cloud cover (Fig. 4). The analysis reveals that the northern and southern hotspots are governed by distinct synoptic paradigms.

In the northern center, compound extreme events are predominantly driven by a mid-latitude high-pressure ridge induced by meridional disturbances of the westerly jet. During hot years, 500-hPa geopotential height exhibits pronounced positive anomalies (maximum increases of 56.3, 45.0, and 47.3 gpm from June to August; Figs. 4a-c), consistently anchored near the climatological axis of the westerlies. This deep ridge configuration strongly resembles circulation patterns triggered by upstream Rossby wave energy dispersion (Teng and Branstator, 2017). As upstream perturbation energy propagates downstream along the jet and becomes quasi-stationary over the mid-to-high latitudes of North America, it establishes a persistent meridional circulation anomaly. The resulting strong subsidence dynamically increases near-surface temperatures via adiabatic warming, while simultaneously suppressing convective moisture condensation.

In stark contrast, compound events in the southern center are dictated by the anomalous westward extension of the NASH. From June to August, significant 500-hPa positive anomalies (up to 55.0 gpm) span the core region and extend continuously eastward toward the western Atlantic (Figs. 4g-i), unequivocally mapping the NASH expansion. Unlike the highly variable wave-driven pattern in the north, the southern circulation anomalies reflect the stable, dominant control of this subtropical system. When this westward-extending ridge intensifies, its massive descending branch directly dominates the southwestern United States and northern Mexico, imposing widespread suppression of precipitation and convection.

A critical, unifying consequence of these dominant high-pressure systems in both regions is the severe depletion of total cloud cover, which inherently links the dynamic circulations to surface UV enhancements. Maximum reductions in total cloud cover reach -13.0 % in the north (Figs. 4d-f) and -12.9 % in the south (Figs. 4j-l). Notably, this overall depletion is primarily driven by the dissipation of low- and mid-level clouds (Figs. S3 and S4). Because low and mid-level clouds exert a

https://doi.org/10.5194/egusphere-2026-4017
Preprint. Discussion started: 28 July 2026

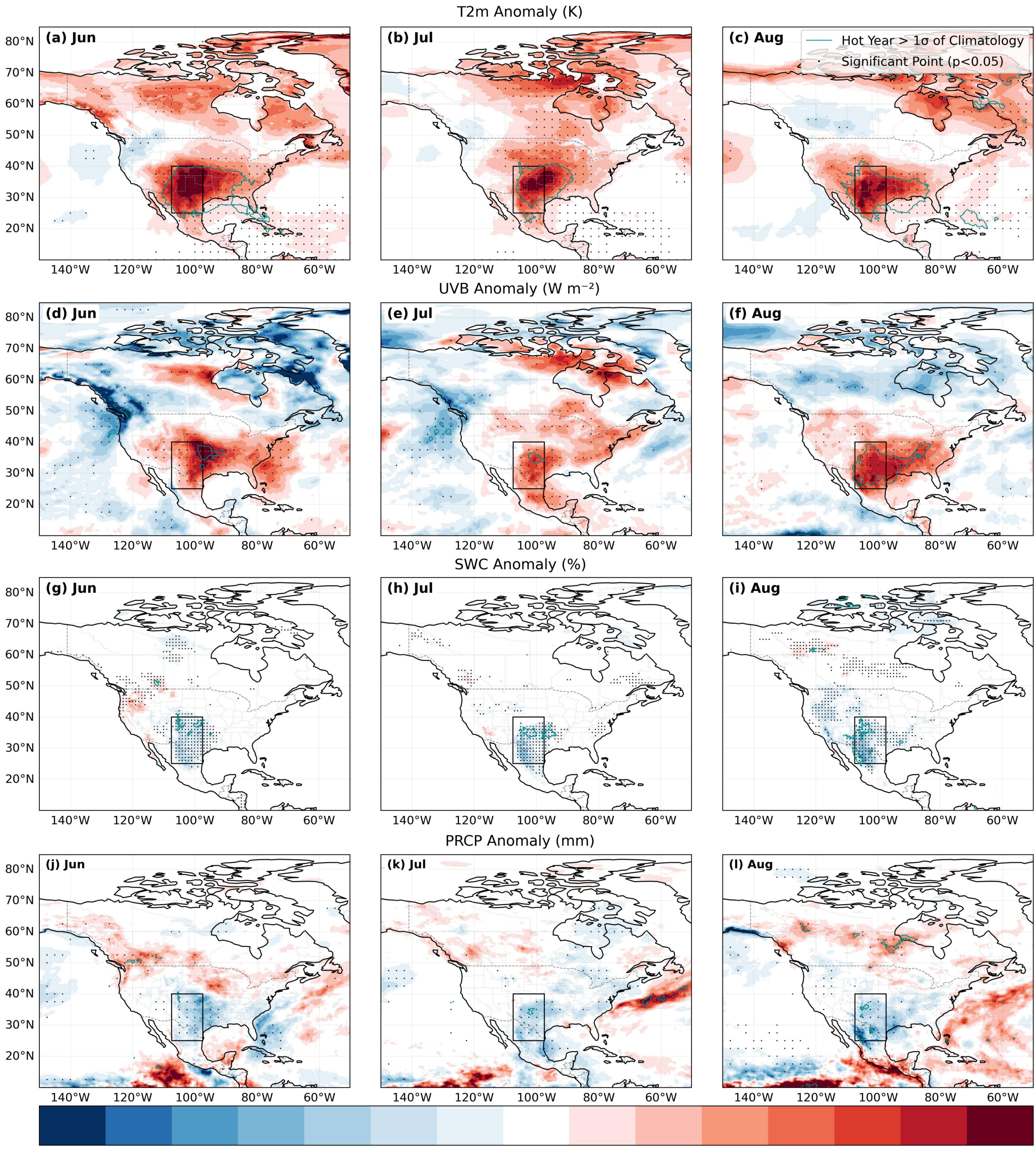

205 **Figure 3: Spatial distributions of composite anomalies during extreme heat events in the southern center for June-August based on ERA5 reanalysis data. Panels (a-c) show 2 m air temperature (T2m) (unit: K), (d-f) surface solar ultraviolet radiation (UVB) (unit:**

W m⁻²), and (j-l) total precipitation (PRCP) (unit: mm), with a color scale ranging from ±2.4. Panels (g-i) show surface volumetric soil water content (SWC) (unit: %), with a color scale ranging from ±80. White denotes zero, and the color scale intervals are evenly spaced. Dotted regions indicate that the composite anomalies are statistically significant at the 95 % confidence level. The dark cyan contour outlines areas where the mean values during hot years exceed ±1 standard deviation of the climatological mean.

solar scattering effect—particularly for UV radiation—that is approximately twice as strong as high clouds (Calbó et al., 2005), their persistent removal drastically amplifies the incoming UV flux reaching the surface. This circulation-induced cloud-clearing effectively completes the physical pathway, directly facilitating the concurrent extreme heat and intense UV exposure.

Taken together, these findings delineate two distinct dynamic blueprints for concurrent heat-UV events: a "westerly disturbance-driven" pattern characterized by strong internal atmospheric wave variability in the north, and a more stable, longer-lasting "westward-extending subtropical high" pattern in the south. Despite their divergent synoptic origins, both paradigms share a fundamental physical mechanism: anomalous anticyclonic systems simultaneously drive surface heating through adiabatic subsidence and amplify UV exposure via severe cloud reduction. Notably, the NASH-driven dynamics in the southern hotspot bear a striking resemblance to the compound heat-UV events reported over the Yangtze Plain in China (Xia et al., 2022). This implies a potential planetary-scale commonality in the mechanisms governing such compound extremes across Northern Hemisphere subtropics, providing a crucial dynamic framework for advancing regional climate prediction and compound risk assessment.

Furthermore, the distinct dynamical natures of these two high-pressure systems are additionally corroborated by anomalies in total column ozone (TCO3). During extreme heat years, the northern hotspot exhibits significant negative TCO3 anomalies (Fig. S5). This column ozone decrease serves as a robust dynamic signature of tropopause lifting driven by deep, persistent mid-latitude ridges (Neu et al., 2014). In contrast, TCO3 anomalies in the southern center remain statistically insignificant (Fig. S6). This neutral column response reflects the differing vertical structure and dynamical origin of the subtropical NASH expansion. Ultimately, these contrasting column ozone footprints further validate the divergent synoptic blueprints governing the two compound heat-UV hotspots.

https://doi.org/10.5194/egusphere-2026-4017
Preprint. Discussion started: 28 July 2026

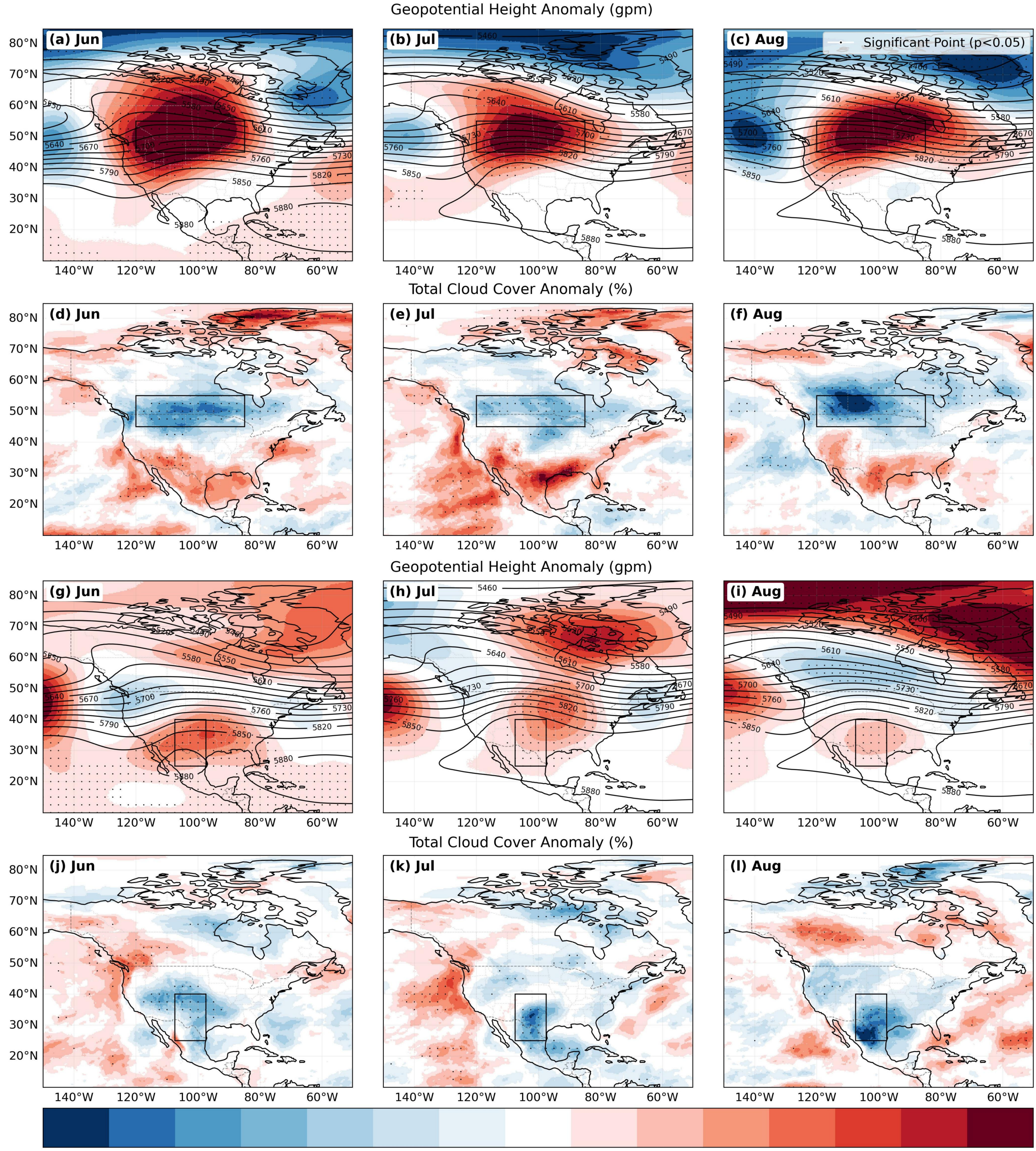

https://doi.org/10.5194/egusphere-2026-4017
Preprint. Discussion started: 28 July 2026

Figure 4: Spatial distributions of composite anomalies associated with extreme heat events during June-August in the northern and southern centers based on ERA5 reanalysis data. Panels (a-c) and (g-i) show 500 hPa geopotential height (unit: gpm), with a color scale ranging from ±40. Black solid contours denote the climatological mean geopotential height for the entire study period (Gaussian smoothed; contour levels from 5460 to 5880 gpm with an interval of 30 gpm). Panels (d-f) and (j-l) show total cloud cover (unit: %), with a color scale ranging from ±12. White indicates zero, and the color scale intervals are evenly spaced. Dotted regions indicate that the composite anomalies are statistically significant at the 95 % confidence level.

3.3 Amplification of Surface Ozone Extremes under Compound Heat-UV Stress

Further analysis demonstrates that concurrent heat-UV extremes incur a substantial "climate penalty" on regional air quality, triggering positive surface ozone anomalies across both the northern and southern hotspots. While this broad response aligns with compound events previously observed over the Yangtze Plain (Xia et al., 2022), the magnitude, spatial continuity, and underlying drivers of the pollution enhancement diverge significantly between the two North American regions.

During summer extreme heat years, surface ozone concentrations surge by up to 15.83 ppbv in the northern center and 15.91 ppbv in the southern center (Fig. 5). However, the southern center emerges as the primary locus of severe pollution amplification. Here, robust ozone enhancements are spatially contiguous and tightly coupled with the core warming region. Conversely, positive anomalies in the northern center are generally weaker, scattered, and largely confined to the periphery of the synoptic ridge.

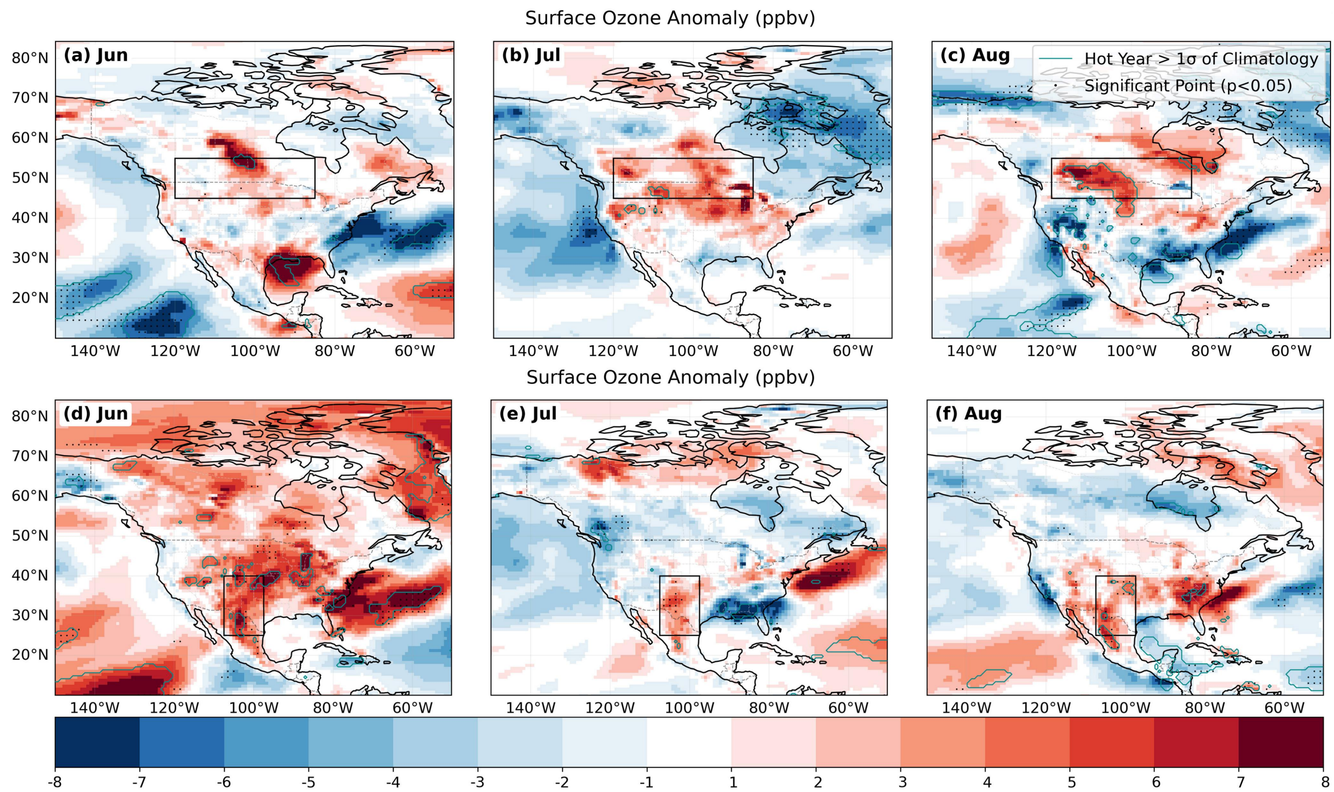

Figure 5: Spatial distributions of composite anomalies in monthly mean surface ozone concentrations (unit: ppbv) associated with extreme heat events during June–August in the northern and southern centers for the period 2003–2022, based on the EAC4

https://doi.org/10.5194/egusphere-2026-4017
Preprint. Discussion started: 28 July 2026

reanalysis dataset. Dotted regions indicate that the composite anomalies are statistically significant at the 95 % confidence level. The dark cyan contour outlines areas where the mean values during hot years exceed ±1 standard deviation of the climatological mean.

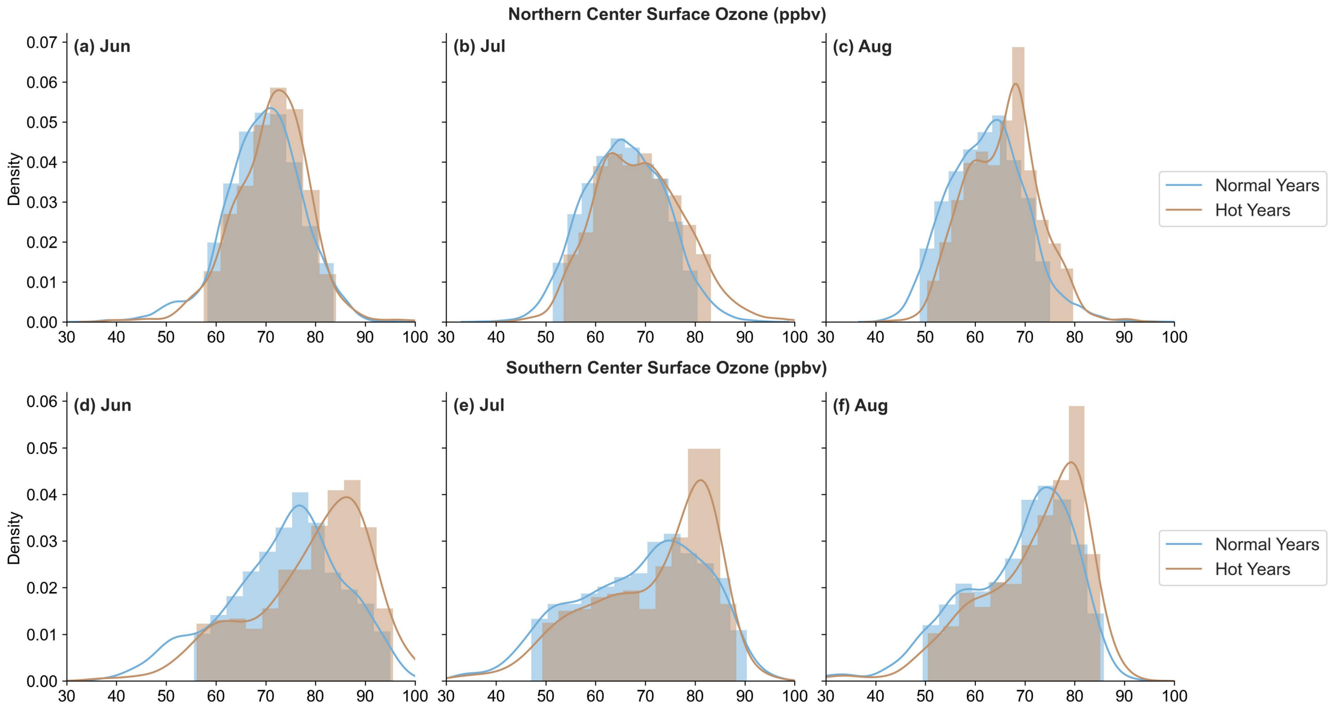

Figure 6: Probability density distributions of monthly mean surface ozone concentrations (unit: ppbv) during June−August for extreme heat years (orange) and normal years (blue) in the northern center (a-c) and southern center (d-f) for the period 2003−2022, based on the EAC4 reanalysis dataset. The histograms display only the high-density concentration ranges, with low-density regions filtered out.

Probability density function (PDF) analysis further unmasks critical differences in how these compound events reshape the distribution of pollution extremes (Fig. 6). In the southern center, the ozone PDF curves for hot years exhibit a pronounced shift toward hazardous concentrations from June to August (Figs. 6d-f). While normal-year ozone levels predominantly fluctuate between 55 and 75 ppbv, compound extremes propel the peak concentration rightward by approximately 10−15 ppbv, drastically increasing the probability of concentrations in the 70−90 ppbv range. This marked rightward skewness indicates that the synergistic heat-UV stress not only elevates baseline ozone levels but also acts as a potent catalyst for extreme, high-impact pollution episodes.

In sharp contrast, the PDF curves for the northern center display only marginal rightward skewness during hot years, lacking a clear enhancement of the high-concentration tail (Figs. 6a-c). This muted distributional response is entirely consistent with the weaker and highly localized surface ozone anomalies observed in this region.

Ultimately, the southern hotspot reveals a fierce spatiotemporal coupling between meteorological extremes and exacerbated surface ozone pollution, establishing it as a critical epicenter for compound environmental risks. Although the environmental

https://doi.org/10.5194/egusphere-2026-4017
Preprint. Discussion started: 28 July 2026

penalty in the northern center is currently less severe, it still warrants vigilant monitoring. These findings carry profound implications for regional public health and ecosystem management. During severe summer heat episodes, mitigation strategies must transcend the traditional focus on heat stress and UV exposure alone. It is imperative to account for the synergistic intensification of photochemical pollution by integrating these coupled meteorological-environmental risks into multi-hazard early warning systems.

3.4 Accelerated Frequency of Compound Extremes under Recent Warming

An analysis of the period from 1980 to 2022 reveals generalized upward trajectories in the occurrence of extreme heat, intense UV radiation, and their compound events across both hotspots (Fig. 7). However, the statistical robustness and magnitude of these decadal trends diverge starkly between the two regions, reflecting differing sensitivities to anthropogenic warming and background natural variability.

In the southern center, the escalation of extremes is stark and statistically robust ($p < 0.05$). Independent extreme heat and intense UV days are surging at rates of 3.35 and 2.23 events per decade, respectively (Figs. 7d-f). Consequently, the frequency of their concurrence has significantly accelerated by 1.29 events per decade. This robust decadal amplification cements the southern region not merely as a spatial hotspot, but as a rapidly intensifying epicenter of compound risks, highly sensitive to ongoing global warming.

Conversely, while the northern center exhibits upward tendencies, none of these trends achieve statistical significance at the 95 % confidence level (Figs. 7a-c). The rates of increase are substantially flatter (1.60, 1.16, and 0.72 events per decade for heat, UV, and compound events, respectively). In this region, pronounced interannual fluctuations overshadow the long-term decadal signal. This high-amplitude internal variability results in a low signal-to-noise ratio, where background natural climate noise currently masks the emergence of a clear anthropogenic warming trend.

Crucially, this stark regional dichotomy in trend detectability perfectly mirrors their distinct synoptic drivers. As established earlier, the southern center is dictated by the NASH. Under global warming, the robust thermodynamic strengthening and systematic westward expansion of subtropical highs provide a persistent, steady dynamical forcing, yielding a prominent and easily detectable upward trend. In sharp contrast, the northern center is governed by mid-latitude westerly disturbances. Planetary wave activity is inherently volatile, heavily modulated by a complex interplay of remote forcings—such as sea surface temperature anomalies, Arctic amplification, and tropical convection. This injects massive internal variability into the northern synoptic environment, leading to more complex long-term signals. This mechanistic interpretation perfectly aligns with broader evidence that trend emergence for extreme events is typically faster and more robust in subtropical regimes compared to the noise-dominated mid-latitudes (Perkins-Kirkpatrick and Lewis, 2020; Grotjahn et al., 2016).

Consequently, the statistically robust intensification of compound events in the southern hotspot signals a rapidly escalating climate-environmental hazard, emphasizing the need for proactive integration into regional risk assessments. In the north, although the secular trend is temporarily obscured by strong internal atmospheric variability, the potential for future

https://doi.org/10.5194/egusphere-2026-4017
Preprint. Discussion started: 28 July 2026

amplification remains high. Recognizing the deep uncertainties surrounding mid-latitude dynamic responses to future warming, continuous monitoring of this northern hotspot is imperative to anticipate and manage latent compound risks.

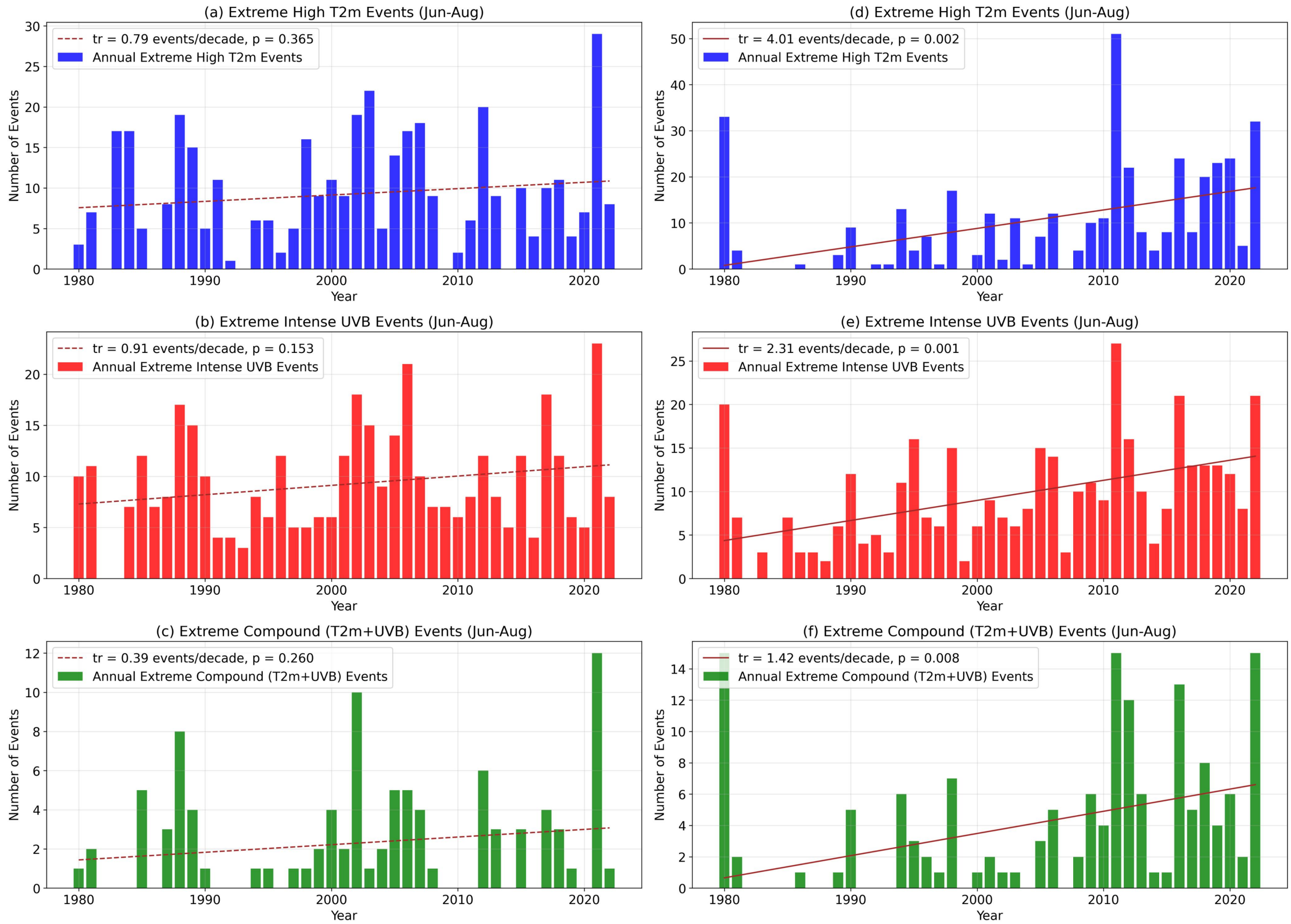

Figure 7: Interannual variations in the annual number of days with extreme heat events, intense UV radiation events, and their compound events during 1980–2022 in the northern center (a-c) and southern center (d-f), based on ERA5 reanalysis data. The label "tr" in the upper-left corner denotes the linear trend in event frequency per decade, and "p" indicates the significance level of the trend test. Linear trend lines that pass the 95 % confidence significance test are shown as solid lines, while those that do not are shown as dashed lines.

4 Conclusions and discussions

This study systematically delineates a severe and rapidly intensifying coupled climate-environmental hazard across North America during the boreal summer. We identify two primary hotspots of concurrent extreme heat and intense UV radiation: a southern center extending from the southwestern United States to northern Mexico, and a northern center spanning central-western Canada to the northwestern United States. These regions exhibit robust and temporally stable positive correlations (up to 0.84) between temperature and UV radiation. Rather than simple meteorological coincidences, these compound

https://doi.org/10.5194/egusphere-2026-4017
Preprint. Discussion started: 28 July 2026

extremes are governed by persistent large-scale anticyclonic circulations that simultaneously enforce subsidence warming, severe soil desiccation (with moisture deficits up to 88 %), and significant cloud depletion (by approximately 13 %), as conceptually summarized in Fig. 8. Crucially, we reveal a distinct regional dichotomy in both dynamical drivers and decadal trajectories. The southern hotspot is anchored by the anomalous westward extension of the NASH. Under ongoing global warming, this NASH-dominated region has experienced a statistically robust and rapid acceleration in compound event frequency (increasing by 1.29 events per decade). In contrast, the northern hotspot is modulated by transient mid-latitude Rossby wave-induced ridging, where the long-term anthropogenic signal is currently overshadowed by strong internal atmospheric variability.

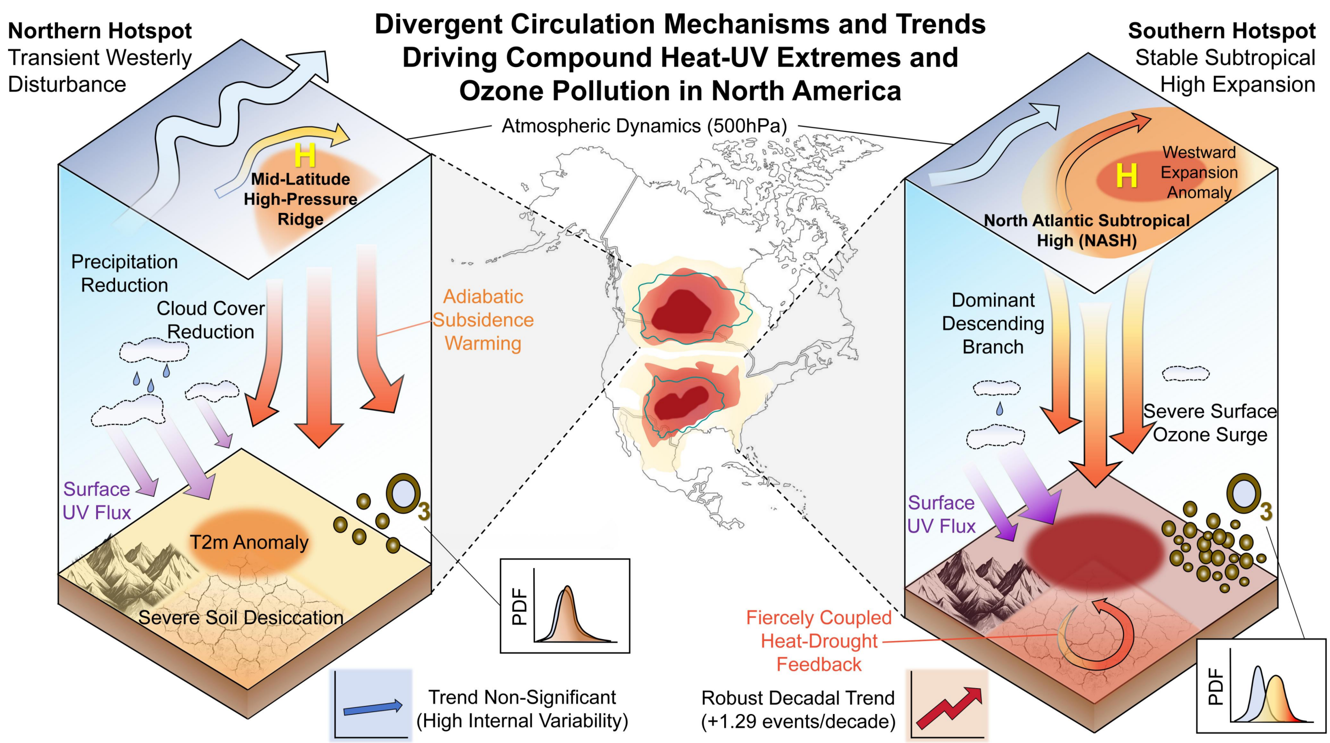

Figure 8: Schematic representation of the physical pathways and ozone pollution impacts of compound heat-UV events in North America. Divergent synoptic circulations — mid-latitude ridges in the north and NASH expansion in the south — drive the two regional hotspots. These anticyclonic systems inherently induce subsidence and severe cloud depletion, synergistically amplifying surface heating and incoming UV radiation. In the southern urbanized hotspot, this combined meteorological forcing dramatically accelerates photochemical reactions with anthropogenic precursors (NOx and VOCs), culminating in severe surface ozone extremes.

Under global climate change, the non-linear amplification of compound extreme events ("1 + 1 > 2") has emerged as a central issue in climate risk research (Zscheischler et al., 2018). While previous literature has extensively documented the co-occurrence of summer heat and drought over North America (Seneviratne et al., 2010; Miralles et al., 2014), this study advances the paradigm. Extending beyond the traditional heat-drought framework, we unmask a tightly coupled hazard chain linking synoptic circulation anomalies to exacerbated air pollution via cloud-radiation feedbacks. Consistent with studies

https://doi.org/10.5194/egusphere-2026-4017
Preprint. Discussion started: 28 July 2026

highlighting the modulation of UV radiation by clouds and aerosols (Barnes et al., 2019), our results demonstrate that large-scale circulation systems systematically regulate cloud cover, transforming thermodynamic extremes into severe radiative and environmental stressors on interannual to decadal timescales (Grotjahn et al., 2016; Li et al., 2012; Li et al., 2019).

The most critical consequence of this coupled hazard chain is the profound "climate penalty" on regional surface ozone, a synergistic effect fundamentally dictated by regional precursor emission inventories. In the relatively "clean" northern center, spanning less densely populated and forested areas, the scarcity of anthropogenic ozone precursors acts as a critical limiting factor. Consequently, despite the thermal and radiative forcing, the photochemical response remains muted and confined to the synoptic periphery. Conversely, the subtropical southern center presents a starkly different environmental baseline where societal ramifications are critically amplified. Here, the meteorological hotspot largely overlaps with major metropolitan areas, such as Los Angeles and Phoenix. In these highly urbanized regions, dense anthropogenic traffic and industrial activities supply a massive inventory of ozone precursors (NOx and VOCs) (Fiore et al., 2012; Schnell and Prather, 2017; Sillman, 1999). During compound events, the urban heat island effect interacts synergistically with large-scale thermal extremes (Zhao et al., 2021; Li and Bou-Zeid, 2013) to exponentially increase VOC emissions and accelerate reaction rates (Jacob and Winner, 2009; Dawson et al., 2007). Simultaneously, circulation-induced clear skies ensure amplified UV radiation that provides excess photons for NOx photolysis (Madronich et al., 2023; Atkinson, 2000). Under this concurrent forcing, the combination of meteorological anomalies and dense urban emissions acts as an explosive catalyst, triggering extreme surface ozone surges of up to 15.9 ppbv and shifting the probability distribution toward hazardous levels by 10–15 ppbv, thereby substantially elevating the risk of severe, high-impact air pollution episodes.

Ultimately, this study advances our mechanistic understanding of compound climate-environmental extremes by providing a vital diagnostic framework for how synoptic circulations simultaneously orchestrate thermal, radiative, and chemical stressors across North America. Building on this foundation, future studies will integrate projection simulations from the latest Coupled Model Intercomparison Project (e.g., CMIP6) with advanced chemical transport models. Such an integrated approach is imperative to quantify the evolving frequency, intensity, and spatial dynamics of these hazard chains under various warming trajectories, ultimately guiding robust environmental adaptation and mitigation strategies.

Code and data availability

The ERA5 and ERA5-Land reanalysis datasets are publicly provided by the European Centre for Medium-Range Weather Forecasts (ECMWF) and can be downloaded from the Copernicus Climate Data Store at https://cds.climate.copernicus.eu/. The CAMS EAC4 atmospheric composition reanalysis dataset is also accessible via the same platform. Detailed descriptions of these datasets are provided in Hersbach et al. (2020), Muñoz-Sabater et al. (2021), and Inness et al. (2019), respectively. The custom analysis code used to produce the results and figures in this study is available from the corresponding author upon reasonable request.

https://doi.org/10.5194/egusphere-2026-4017
Preprint. Discussion started: 28 July 2026

Author contributions

BB and YX conceived the study and developed the methodology. BB performed data curation, formal analysis, software development, validation and visualization, and drafted the original manuscript. YX and FX supervised the project, provided research resources, and revised and edited the manuscript. All authors contributed to the interpretation of results and approved the final version.

Competing interests

The authors declare that they have no conflict of interest.

Financial support

This work was supported by the financial support of National Key Research and Development Program of China (No. 2022YFF0801701) and National Natural Science Foundation of China (Grants 42375070).

References

Adrian, R., Craig, M., Degvold, F., Ebi, K. L., Frieler, K., Jamshed, A., McMillan, J., Mechler, R., New, M., Simpson, N., and Stevens, N.: Climate Change 2022 – Impacts, Adaptation and Vulnerability: Summary for Policymakers, Project Report, Intergovernmental Panel on Climate Change (IPCC), https://library.arcticportal.org/id/eprint/2000, 2022.

Afroz, M., Chen, G., and Anandhi, A.: Drought-and heatwave-associated compound extremes: A review of hotspots, variables, parameters, drivers, impacts, and analysis frameworks, Front. Earth Sci., 10, 914437, https://doi.org/10.3389/feart.2022.914437, 2023.

Anderson, G. B., and Bell, M. L.: Heat waves in the United States: mortality risk during heat waves and effect modification by heat wave characteristics in 43 US communities, Environ. Health Perspect., 119, 210, https://doi.org/10.1289/ehp.1002312, 2010.

Allen, C. D., Macalady, A. K., Chenchouni, H., Bachelet, D., McDowell, N., Vennetier, M., Kitzberger, T., Rigling, A., Breshears, D. D., Hogg, E. H., Gonzalez, P., Fensham, R., Zhang, Z., Castro, J., Demidova, N., Lim, J.-H., Allard, G., Running, S. W., Semerci, A., and Cobb, N.: A global overview of drought and heat-induced tree mortality reveals emerging climate change risks for forests, For. Ecol. Manage., 259, 660–684, https://doi.org/10.1016/j.foreco.2009.09.001, 2010.

Adams, R. E., Lee, C. C., Smith, E. T., and Sheridan, S. C.: The relationship between atmospheric circulation patterns and extreme temperature events in North America, Int. J. Climatol., 41, 92–103, https://doi.org/10.1002/joc.6610, 2021.

Atkinson, R.: Atmospheric chemistry of VOCs and NOx, Atmos. Environ., 34, 2063–2101, https://doi.org/10.1016/S1352-2310(99)00460-4, 2000.

https://doi.org/10.5194/egusphere-2026-4017
Preprint. Discussion started: 28 July 2026

Bornman, J. F., Barnes, P. W., Robson, T. M., Robinson, S. A., Jansen, M. A. K., Ballaré, C. L., and Flint, S. D.: Linkages between stratospheric ozone, UV radiation and climate change and their implications for terrestrial ecosystems, Photochem. Photobiol. Sci., 18, 681–716, https://doi.org/10.1039/c8pp90061b, 2019.

Ballaré, C. L., Caldwell, M. M., Flint, S. D., Robinson, S. A., and Bornman, J. F.: Effects of solar ultraviolet radiation on terrestrial ecosystems. Patterns, mechanisms, and interactions with climate change, Photochem. Photobiol. Sci., 10, 226–241, https://doi.org/10.1039/c0pp90035d, 2011.

Bais, A. F., McKenzie, R. L., Bernhard, G., Aucamp, P. J., Ilyas, M., Madronich, S., and Tourpali, K.: Ozone depletion and climate change: impacts on UV radiation, Photochem. Photobiol. Sci., 14, 19–52, https://doi.org/10.1039/c4pp90032d, 2015.

Barnes, P. W., Williamson, C. E., Lucas, R. M., Robinson, S. A., Madronich, S., Paul, N. D., Bornman, J. F., Bais, A. F., Sulzberger, B., Wilson, S. R., Andrady, A. L., McKenzie, R. L., Neale, P. J., Austin, A. T., Bernhard, G., Solomon, K. R., Neale, R. E., Young, A. R., Norval, M., Rhodes, L. E., Hylander, S., and Zepp, R. G.: Ozone depletion, ultraviolet radiation, climate change and prospects for a sustainable future, Nat. Sustain., 2, 569–579, https://doi.org/10.1038/s41893-019-0314-2, 2019.

Campbell, S., Remenyi, T. A., White, C. J., and Johnston, F. H.: Heatwave and health impact research: A global review, Health Place, 53, 210–218, https://doi.org/10.1016/j.healthplace.2018.08.017, 2018.

Coumou, D. and Rahmstorf, S.: A decade of weather extremes, Nat. Clim. Change, 2, 491–496, https://doi.org/10.1038/nclimate1452, 2012.

Chiang, F., Mazdiyasni, O., and AghaKouchak, A.: Evidence of anthropogenic impacts on global drought frequency, duration, and intensity, Nat. Commun., 12, 2754, https://doi.org/10.1038/s41467-021-22314-w, 2021.

Calbó, J., Pages, D., and González, J. A.: Empirical studies of cloud effects on UV radiation: A review, Rev. Geophys., 43, https://doi.org/10.1029/2004RG000155, 2005.

Dyson, T.: World food trends and prospects to 2025, Proc. Natl. Acad. Sci. U.S.A., 96, 5929–5936, https://doi.org/10.1073/pnas.96.11.5929, 1999.

Dawson, J. P., Adams, P. J., and Pandis, S. N.: Sensitivity of ozone to summertime climate in the eastern USA: A modeling case study, Atmos. Environ., 41, 1494–1511, https://doi.org/10.1016/j.atmosenv.2006.10.033, 2007.

Fischer, E. M. and Knutti, R.: Observed heavy precipitation increase confirms theory and early models, Nat. Clim. Change, 6, 986–991, https://doi.org/10.1038/nclimate3110, 2016.

Fiore, A. M., Naik, V., Spracklen, D. V., Steiner, A., Unger, N., Prather, M., Bergmann, D., Cameron-Smith, P. J., Cionni, I., Collins, W. J., Dalsøren, S., Eyring, V., Folberth, G. A., Ginoux, P., Horowitz, L. W., Josse, B., Lamarque, J.-F., MacKenzie, I. A., Nagashima, T., O'Connor, F. M., Righi, M., Rumbold, S. T., Shindell, D. T., Skeie, R. B., Sudo, K., Szopa, S., Takemura, T., and Zeng, G.: Global air quality and climate, Chem. Soc. Rev., 41, 6663–6683, https://doi.org/10.1039/c2cs35095e, 2012.

Gulev, S. K., Thorne, P. W., Ahn, J., Dentener, F. J., Domingues, C. M., Gerland, S., Gong, D., Kaufman, D. S., Nnamchi, H. C., Quaas, J., Rivera, J. A., Sathyendranath, S., Smith, S. L., Trewin, B., von Schuckmann, K., Vose, R. S., Hawkins, E., and

https://doi.org/10.5194/egusphere-2026-4017
Preprint. Discussion started: 28 July 2026

the Intergovernmental Panel on Climate Change: Changing state of the climate system, in: Climate Change 2021: The Physical Science Basis, Contribution of Working Group I to the Sixth Assessment Report of the Intergovernmental Panel on Climate Change, Cambridge University Press, Cambridge, United Kingdom and New York, NY, USA, 287–422, https://doi.org/10.1017/9781009157896.004, 2021.

Grotjahn, R., Black, R., Leung, R., Wehner, M. F., Barlow, M., Bosilovich, M., Gershunov, A., Gutowski, W. J., Gyakum, J. R., Katz, R. W., Lee, Y.-Y., Lim, Y.-K., and Prabhat: North American extreme temperature events and related large scale meteorological patterns: a review of statistical methods, dynamics, modeling, and trends, Clim. Dyn., 46, 1151–1184, https://doi.org/10.1007/s00382-015-2638-6, 2016.

Graff Zivin, J. and Neidell, M.: Temperature and the allocation of time: Implications for climate change, J. Labor Econ., 32, 1–26, https://doi.org/10.1086/671766, 2014.

Häder, D. P., Williamson, C. E., Wängberg, S.-Å., Rautio, M., Rose, K. C., Gao, K., Helbling, E. W., Sinha, R. P., and Worrest, R.: Effects of UV radiation on aquatic ecosystems and interactions with other environmental factors, Photochem. Photobiol. Sci., 14, 108–126, https://doi.org/10.1039/c4pp90035a, 2015.

Hersbach, H., Bell, B., Berrisford, P., Hirahara, S., Horányi, A., Muñoz-Sabater, J., Nicolas, J., Peubey, C., Radu, R., Schepers, D., Simmons, A., Soci, C., Abdalla, S., Abellan, X., Balsamo, G., Bechtold, P., Biavati, G., Bidlot, J., Bonavita, M., De Chiara, G., Dahlgren, P., Dee, D., Diamantakis, M., Dragani, R., Flemming, J., Forbes, R., Fuentes, M., Geer, A., Haimberger, L., Healy, S., Hogan, R. J., Hólm, E., Janisková, M., Keeley, S., Laloyaux, P., Lopez, P., Lupu, C., Radnoti, G., de Rosnay, P., Rozum, I., Vamborg, F., Villaume, S., and Thépaut, J. N.: The ERA5 global reanalysis, Copernicus Climate Data Store (CDS) [data set], https://doi.org/10.1002/qj.3803, 2020.

Inness, A., Ades, M., Agustí-Panareda, A., Barré, J., Benedictow, A., Blechschmidt, A. M., Domínguez, J. J., Engelen, R., Eskes, H., Flemming, J., Huijnen, V., Jones, L., Kipling, Z., Massart, S., Parrington, M., Peuch, V.-H., Razinger, M., Remy, S., Schulz, M., and Suttie, M.: The CAMS reanalysis of atmospheric composition, Copernicus Atmosphere Data Store (ADS) [data set], https://doi.org/10.5194/acp-19-3515-2019, 2019.

Jones, B., O'Neill, B. C., McDaniel, L., McGinnis, S., Mearns, L. O., and Tebaldi, C.: Future population exposure to US heat extremes, Nat. Clim. Change, 5, 652–655, https://doi.org/10.1038/nclimate2631, 2015.

Jacob, D. J. and Winner, D. A.: Effect of climate change on air quality, Atmos. Environ., 43, 51–63, https://doi.org/10.1016/j.atmosenv.2008.09.051, 2009.

Knowlton, K., Rotkin-Ellman, M., King, G., Margolis, H. G., Smith, D., Solomon, G., Trent, R., and English, P.: The 2006 California heat wave: impacts on hospitalizations and emergency department visits, Environ. Health Perspect., 117, 61, https://doi.org/10.1289/ehp.11594, 2008.

Li, L., Li, W., and Kushnir, Y.: Variation of the North Atlantic subtropical high western ridge and its implication to Southeastern US summer precipitation, Clim. Dyn., 39, 1401–1412, https://doi.org/10.1007/s00382-011-1214-y, 2012.

Li, W., Zou, T., Li, L., Deng, Y., Sun, V. T., Zhang, Q., Jiang, L., and Setoguchi, S.: Impacts of the North Atlantic subtropical high on interannual variation of summertime heat stress over the conterminous United States, Clim. Dyn., 53, 3345–3359, https://doi.org/10.1007/s00382-019-04708-1, 2019.

Loikith, P. C. and Broccoli, A. J.: Characteristics of observed atmospheric circulation patterns associated with temperature extremes over North America, J. Clim., 25, 7266–7281, https://doi.org/10.1175/JCLI-D-11-00709.1, 2012.

Liaqat, W., Altaf, M. T., Barutçular, C., Nawaz, H., Ullah, I., Basit, A., and Mohamed, H. I.: Ultraviolet-B radiation in relation to agriculture in the context of climate change: a review, Cereal Res. Commun., 52, 1–24, https://doi.org/10.1007/s42976-023-00375-5, 2024.

Lu, Y., Li, M., Zhou, Y., Zhang, H., Wang, W., Huang, X., and Li, S.: Vegetation-atmosphere feedbacks exacerbate ozone pollution during compound heatwave and drought in the northern hemisphere, J. Geophys. Res. Atmos., 131, e2025JD044433, https://doi.org/10.1029/2025JD044433, 2026.

Liao, Z., Zhang, J., Gao, M., and Ma, Z.: Widespread stratospheric intrusion influence on summer ozone pollution over China revealed by multi-site ozonesonde and validated EAC4 reanalysis, Atmos. Chem. Phys., 25, 14865–14877, 2025.

Li, D. and Bou-Zeid, E.: Synergistic interactions between urban heat islands and heat waves: The impact in cities is larger than the sum of its parts, J. Appl. Meteorol. Climatol., 52, 2051–2064, https://doi.org/10.1175/JAMC-D-13-02.1, 2013.

Miralles, D. G., Teuling, A. J., Van Heerwaarden, C. C., and Vilà-Guerau de Arellano, J.: Mega-heatwave temperatures due to combined soil desiccation and atmospheric heat accumulation, Nat. Geosci., 7, 345–349, https://doi.org/10.1038/ngeo2141, 2014.

Madronich, S., Sulzberger, B., Longstreth, J. D., Schikowski, T., Andersen, M. S., Solomon, K. R., and Wilson, S. R.: Changes in tropospheric air quality related to the protection of stratospheric ozone in a changing climate, Photochem. Photobiol. Sci., 22, 1129–1176, https://doi.org/10.1007/s43630-023-00369-6, 2023.

Muñoz-Sabater, J., Dutra, E., Agustí-Panareda, A., Albergel, C., Arduini, G., Balsamo, G., Boussetta, S., Choulga, M., Harrigan, S., Hersbach, H., Martens, B., Miralles, D. G., Piles, M., Rodríguez-Fernández, N. J., Zsoter, E., Buontempo, C., and Thépaut, J. N.: ERA5-Land: A state-of-the-art global reanalysis dataset for land applications, Copernicus Climate Data Store (CDS) [data set], https://doi.org/10.5194/essd-13-4349-2021, 2021.

Niu, Y., Li, Y., Xia, Y., and Xie, F.: Sensitivity of ground-level ozone to surface elevation in CMIP6: Role of stratosphere-troposphere exchange, Glob. Planet. Change, 105054, 2025.

Neu, J. L., Flury, T., Manney, G. L., Santee, M. L., Livesey, N. J., and Worden, J.: Tropospheric ozone variations governed by changes in stratospheric circulation, Nat. Geosci., 7, 340–344, https://doi.org/10.1038/ngeo2138, 2014.

Perkins-Kirkpatrick, S. E. and Lewis, S. C.: Increasing trends in regional heatwaves, Nat. Commun., 11, 3357, https://doi.org/10.1038/s41467-020-16970-7, 2020.

Perkins, S. E., Alexander, L. V., and Nairn, J. R.: Increasing frequency, intensity and duration of observed global heatwaves and warm spells, Geophys. Res. Lett., 39, https://doi.org/10.1029/2012GL053361, 2012.

Papalexiou, S. M. and Montanari, A.: Global and regional increase of precipitation extremes under global warming, Water Resour. Res., 55, 4901–4914, https://doi.org/10.1029/2018WR024067, 2019.

Perkins, S. E.: A review on the scientific understanding of heatwaves—Their measurement, driving mechanisms, and changes at the global scale, Atmos. Res., 164–165, 242–267, https://doi.org/10.1016/j.atmosres.2015.05.014, 2015.

Philip, S. Y., Kew, S. F., Van Oldenborgh, G. J., Anslow, F. S., Seneviratne, S. I., Vautard, R., Coumou, D., Ebi, K. L., Arrighi, J., Singh, R., van Aalst, M., and Otto, F. E. L.: Rapid attribution analysis of the extraordinary heat wave on the Pacific coast of the US and Canada in June 2021, Earth Syst. Dyn., 13, 1689–1713, https://doi.org/10.5194/esd-13-1689-2022, 2022.

Robson, T. M., Pieristè, M., Durand, M., Kotilainen, T. K., and Aphalo, P. J.: The benefits of informed management of sunlight in production greenhouses and polytunnels, Plants People Planet, 4, 314–325, https://doi.org/10.1002/ppp3.10258, 2022.

Schlenker, W. and Roberts, M. J.: Nonlinear temperature effects indicate severe damages to US crop yields under climate change, Proc. Natl. Acad. Sci. U.S.A., 106, 15594–15598, https://doi.org/10.1073/pnas.0906865106, 2009.

Seneviratne, S. I., Corti, T., Davin, E. L., Hirschi, M., Jaeger, E. B., Lehner, I., Orlowsky, B., and Teuling, A. J.: Investigating soil moisture-climate interactions in a changing climate: A review, Earth-Sci. Rev., 99, 125–161, https://doi.org/10.1016/j.earscirev.2010.02.004, 2010.

Schnell, J. L. and Prather, M. J.: Co-occurrence of extremes in surface ozone, particulate matter, and temperature over eastern North America, Proc. Natl. Acad. Sci. U.S.A., 114, 2854–2859, https://doi.org/10.1073/pnas.1614453114, 2017.

Staten, P. W., Lu, J., Grise, K. M., Davis, S. M., and Birner, T.: Re-examining tropical expansion, Nat. Clim. Change, 8, 768–775, https://doi.org/10.1038/s41558-018-0246-2, 2018.

Sillman, S.: The relation between ozone, NOx and hydrocarbons in urban and polluted rural environments, Atmos. Environ., 33, 1821–1845, https://doi.org/10.1016/S1352-2310(98)00345-8, 1999.

Teng, H., Branstator, G., Wang, H., Meehl, G. A., and Washington, W. M.: Probability of US heat waves affected by a subseasonal planetary wave pattern, Nat. Geosci., 6, 1056–1061, https://doi.org/10.1038/ngeo1988, 2013.

Teng, H. and Branstator, G.: Causes of extreme ridges that induce California droughts, J. Clim., 30, 1477–1492, https://doi.org/10.1175/JCLI-D-16-0524.1, 2017.

USGCRP: Fourth National Climate Assessment, U.S. Global Change Research Program, Washington, DC, USA, https://www.350montana.org/wp-content/uploads/2019/12/nwe/NationalClimateAssessment.pdf, 2018.

Westerling, A. L., Hidalgo, H. G., Cayan, D. R., and Swetnam, T. W.: Warming and earlier spring increase western US forest wildfire activity, Science, 313, 940–943, https://doi.org/10.1126/science.1128834, 2006.

World Health Organization: Radiation: The known health effects of ultraviolet radiation, World Health Organization, https://www.who.int/zh/news-room/questions-and-answers/item/radiation-the-known-health-effects-of-ultraviolet-radiation, 2017.

Williamson, C. E., Zepp, R. G., Lucas, R. M., Madronich, S., Austin, A. T., Ballaré, C. L., Norval, M., Sulzberger, B., Bais, A. F., McKenzie, R. L., Robinson, S. A., Häder, D.-P., Paul, N. D., and Bornman, J. F.: Solar ultraviolet radiation in a changing climate, Nat. Clim. Change, 4, 434–441, https://doi.org/10.1038/nclimate2225, 2014.

Wang, X., Hou, X., Zhao, T., Zhang, Y., Pandey, A., and Jin, Y.: Characteristics and identification of stratospheric ozone slanted intrusion into the troposphere in the BTH region, Atmos. Res., 108497, 2025.

Xia, Y., Hu, Y., Huang, Y., Bian, J., Zhao, C., Wei, J., Yan, L., Li, Q., Liu, C., and Lin, J.: Concurrent hot extremes and high ultraviolet radiation in summer over the Yangtze Plain and their possible impact on surface ozone, Environ. Res. Lett., 17, 064001, https://doi.org/10.1088/1748-9326/ac6c3c, 2022.

Xia, Y., Hu, Y., Huang, Y., Bian, J., and Zhao, C.: Stratospheric ozone loss-induced cloud effects lead to less surface ultraviolet radiation over the Siberian Arctic in spring, Environ. Res. Lett., 16, 084057, https://doi.org/10.1088/1748-9326/ac18e9, 2021a.

Xia, Y., Hu, Y., Huang, Y., Zhao, C., Xie, F., and Yang, Y.: Significant contribution of severe ozone loss to the Siberian-Arctic surface warming in spring 2020, Geophys. Res. Lett., 48, e2021GL092509, https://doi.org/10.1029/2021GL092509, 2021b.

Xie, F., Li, J., Tian, W., Fu, Q., Jin, F. F., Hu, Y., Zhang, J., Wang, W., Sun, C., Feng, J., Yang, Y., and Ding, R.: A connection from Arctic stratospheric ozone to El Niño-Southern oscillation, Environ. Res. Lett., 11, 124026, https://doi.org/10.1088/1748-9326/11/12/124026, 2016.

Xie, F., Li, J., Zhang, J., Tian, W., Hu, Y., Zhao, S., Sun, C., Ding, R., Feng, J., and Yang, Y.: Variations in North Pacific sea surface temperature caused by Arctic stratospheric ozone anomalies, Environ. Res. Lett., 12, 114023, https://doi.org/10.1088/1748-9326/aa9005, 2017.

Xie, F., Zhang, J., Li, X., Li, J., Wang, T., and Xu, M.: Independent and joint influences of eastern Pacific El Niño-southern oscillation and quasi-biennial oscillation on Northern Hemispheric stratospheric ozone, Int. J. Climatol., 40, 5289–5307, https://doi.org/10.1002/joc.6519, 2020.

Xiang, X., Xie, F., and Xia, Y.: Quasi-decadal oscillation of concurrent cold extremes and intense surface ultraviolet radiation events over the East European Plain, Environ. Res. Lett., 20, 064041, https://doi.org/10.1088/1748-9326/adda66, 2025.

Zscheischler, J., Westra, S., Van Den Hurk, B. J. J. M., Seneviratne, S. I., Ward, P. J., Pitman, A., AghaKouchak, A., Bresch, D. N., Leonard, M., Wahl, T., and Zhang, X.: Future climate risk from compound events, Nat. Clim. Change, 8, 469–477, https://doi.org/10.1038/s41558-018-0156-3, 2018.

Zhao, R. and Yang, Y.: Expanding compound heat and ultraviolet radiation stress amplifies exposure risks for elderly populations, Commun. Earth Environ., 6, 064041, https://doi.org/10.1038/s43247-025-03070-x, 2025.

Zhao, L., Oleson, K., Bou-Zeid, E., Krayenhoff, E. S., Bray, A., Zhu, Q., Zheng, Z., Chen, C., and Oppenheimer, M.: Global multi-model projections of local urban climates, Nat. Clim. Change, 11, 152–157, https://doi.org/10.1038/s41558-020-00958-8, 2021.

Zhang, Y., Tian, Q., Feng, X., Hu, W., Ma, P., Xin, J., Li, L., Wang, S., and Zheng, C.: Modification effects of ambient temperature on ozone-mortality relationships in Chengdu, China, Environ. Sci. Pollut. Res., 29, 73011–73019, https://doi.org/10.1007/s11356-022-20843-5, 2022.